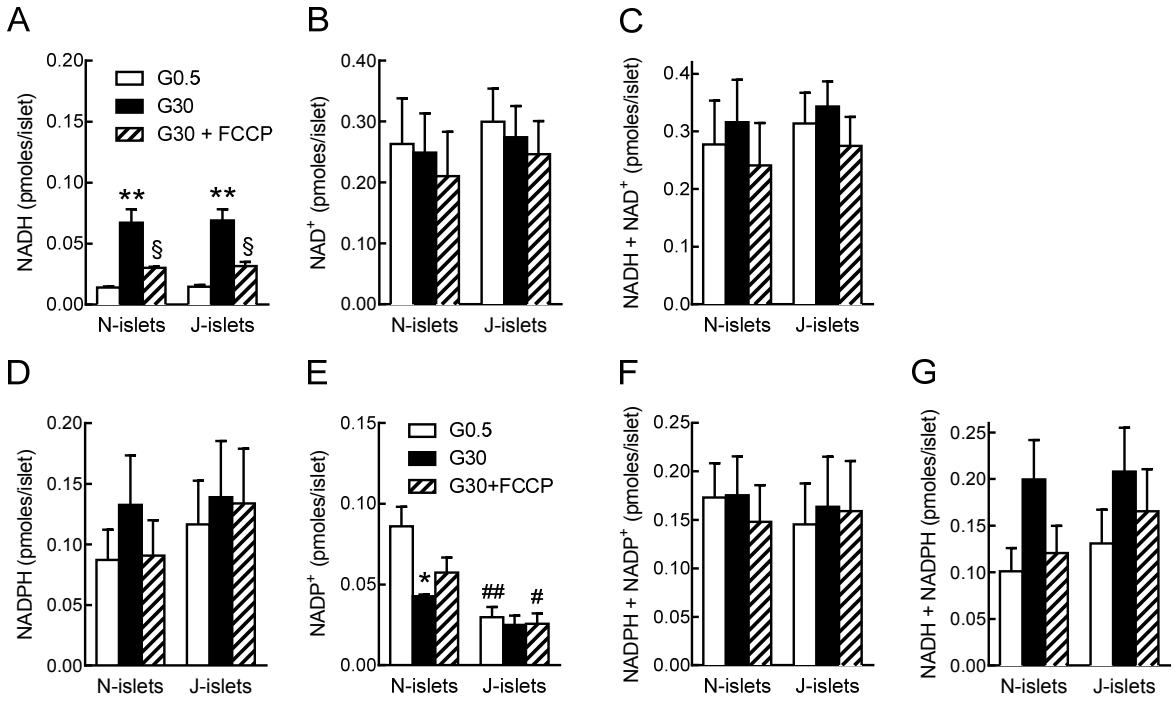

Figure S1. Effects of glucose and FCCP on pyridine nucleotides in islets from C57BL/6N and C57BL/6J mice. Related to figure 1.

A-G, after 40 min preincubation in G0.5, N- and J-islets were incubated 15 min in G0.5, G30, or G30 plus 10 µmol/l FCCP. A-C, NADH and NAD^+ were measured in whole islet extracts and the sum NADH + NAD^+ was computed. D-F, NADPH and $NADP^+$ were measured in whole islet extracts and the sum NADPH + $NADP^+$ was computed. G, the level of NADH + NADPH per islet was estimated by summing data from panels B and E obtained in different islet preparations. Data are means ± SEM for 3 islet preparations. * $P<0.01$, ** $P<0.001$ *vs.* G0.5; § $P<0.01$ *vs.* G30; # $P<0.05$ and ## $P<0.001$ *vs.* N-islets.

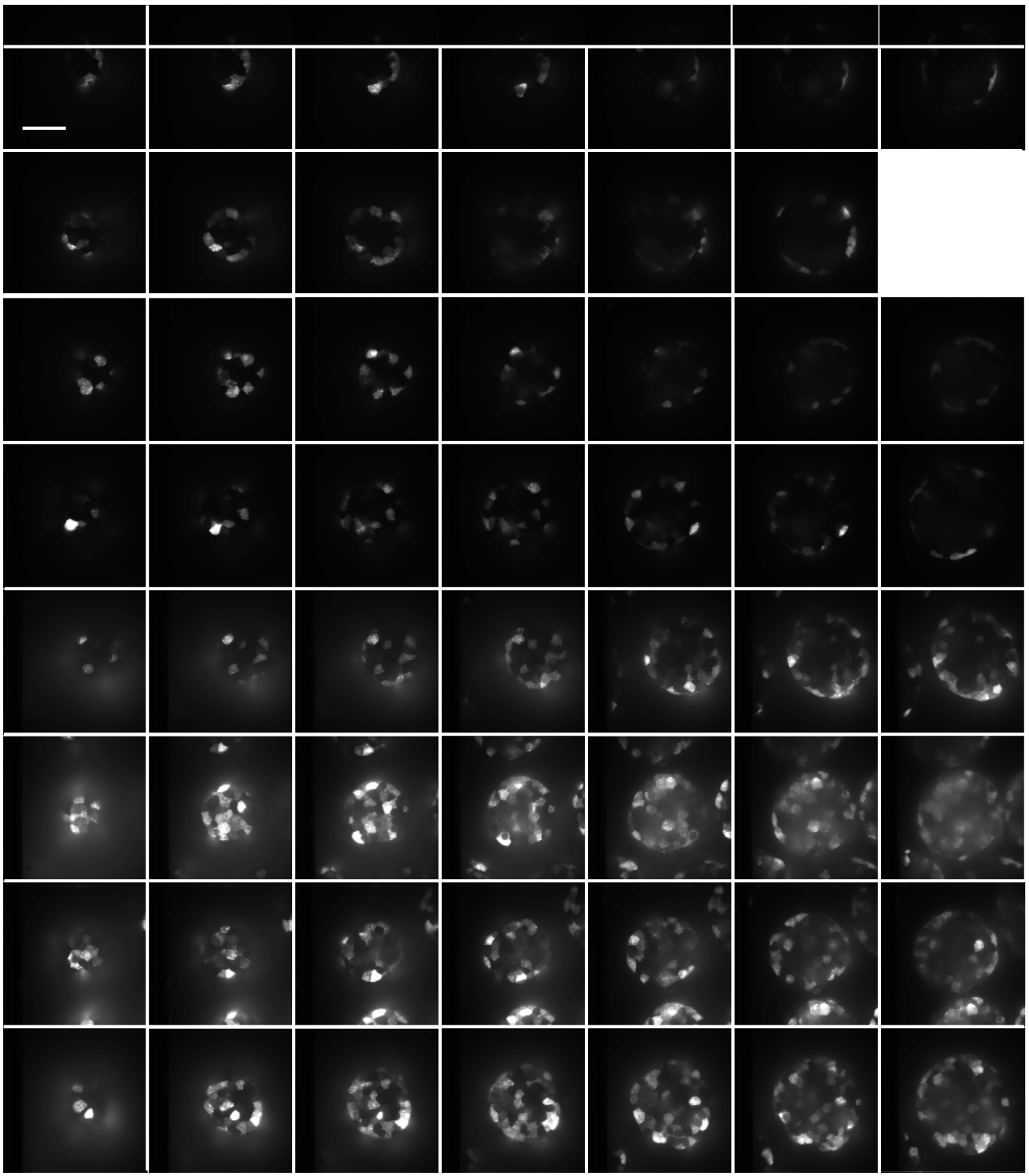

Figure S2. Impact of gentle islet trypsinization on adenovirus-mediated gene expression.

Related to figure 1.

Confocal imaging of mCherry expression (λex 561 nm; λem 635-685 nm) in J-islets infected with Ad-mCherry-NNT under normal conditions (first 4 rows) or after gentle trypsinization of the islets (last 4 rows) and 96 h culture. Each row displays different focal planes from the same islet, from the bottom of the islet on the left. Images were acquired for 1 sec with a 40x objective and an Evolve 512 EMCCD camera in the 5 MHz Standard acquisition mode. The stronger background in gently trypsinized islets resulted from the higher fluorescence of out-of-focus islet cells. The data are representative for two experiments. Scale bar, 50 μm.

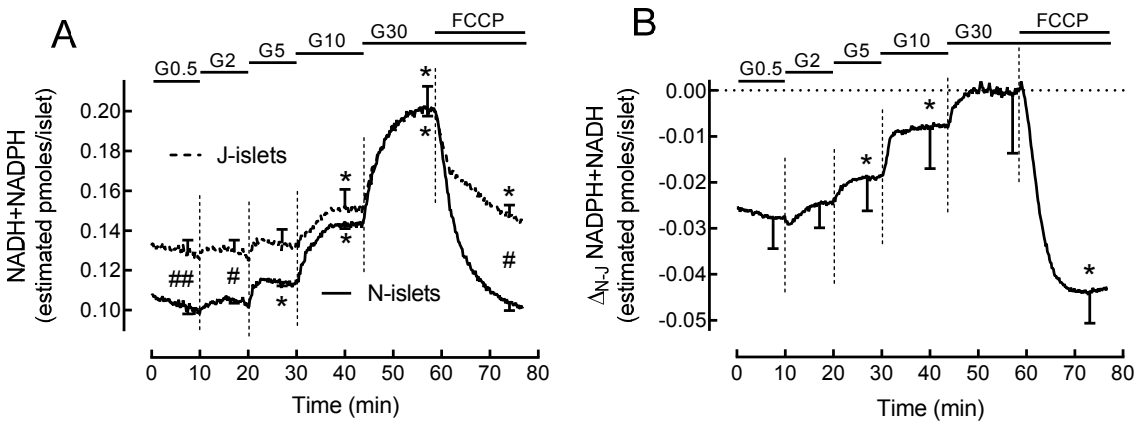

Figure S3. Simulation of glucose-induced changes in NADPH+NADH levels and impact of NNT on islet NADPH levels. Related to figure 1.

A, glucose-induced changes in NADPH+NADH content in N- and J-islets were estimated by normalizing NAD(P)H autofluorescence levels shown in figures 1B to the sum NADPH+NADH in G0.5 and G30 in each islet type (Suppl. Fig. 1G). B, the difference between both traces was then computed. Data are means ± SEM for 3 islet preparations. * P<0.001 *vs.* G0.5; # P<0.05, ## P<0.01 *vs.* N-islets. B, * P<0.05 *vs.* G0.5 (one-way ANOVA + test of Bonferroni)

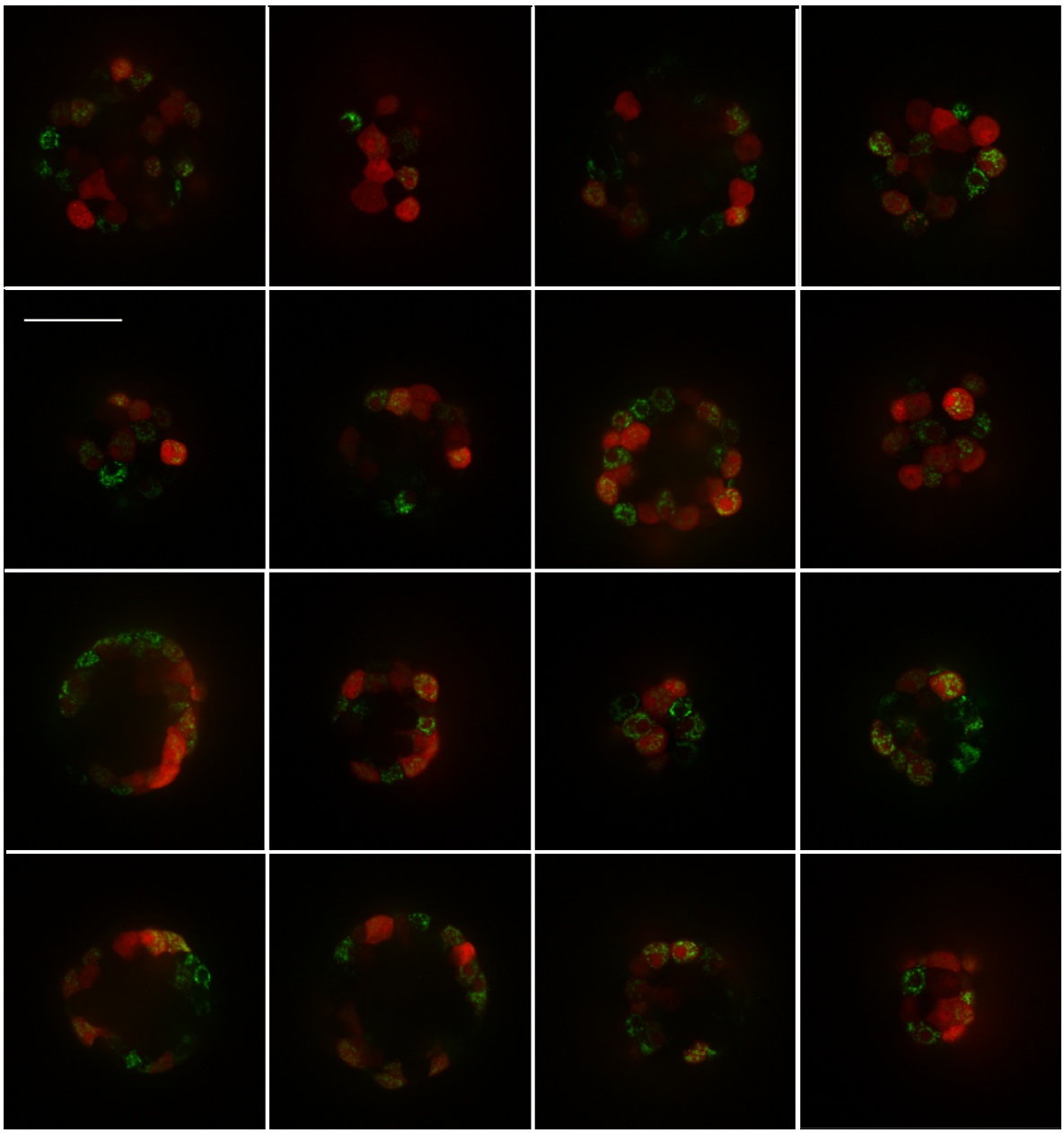

Figure S4. Expression of mt-GRX1-roGFP2 in mouse islet beta-cells. Related to figure 2. Confocal imaging of Ds-Red (λex 561 nm; λem 635-685 nm, gray fluorescence converted to red pseudocolour) and mt-GRX1-roGFP2 (λex 491 nm; λem 503-552 nm, gray fluorescence converted to green pseudocolour) in C57BL/6 mouse islets co-infected with Ad-RIP-DsRed and Ad-CMV-mt-GRX1-roGFP2 followed by 48h of culture. Images were acquired at room temperature for 1 sec with a 40x objective and a Coolsnap™ EZ EMCCD camera (Photometrics, Tucson, AZ), using Metamorph (Molecular Devices). The data are representative for 21 confocal sections from 5 J-islets (two upper rows) and 13 sections from 4 N-islets (two lower rows). Scale bar, 50 μm. On average, 70% of mt-GRX1-roGFP2-positive cells were also DsRed-positive, while 79% of DsRed-positive cells were also mt-GRX1-roGFP2 positive.

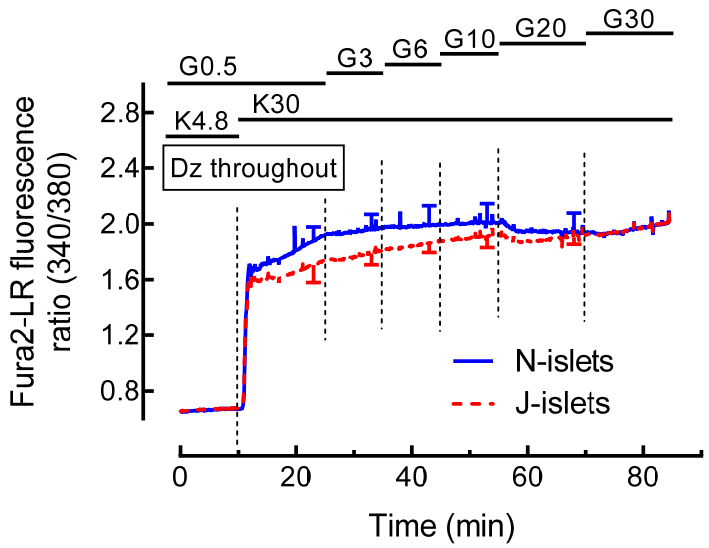

Figure S5. Glucose-induced changes in $[Ca^{2+}]_i$ in N- and J-islets under depolarizing conditions. Related to figure 5.

After loading for 2 h with 2 µmol/l fura2-LR, N- and J-islets were perifused at increasing glucose concentrations under depolarizing conditions (Kn, n mmol/l extracellular K^+; Dz, 250 µmol/l diazoxide). The fura2-LR fluorescence ratio was recorded simultaneously in J- and N-islets. Data are means ± SEM for 3 islet preparations.

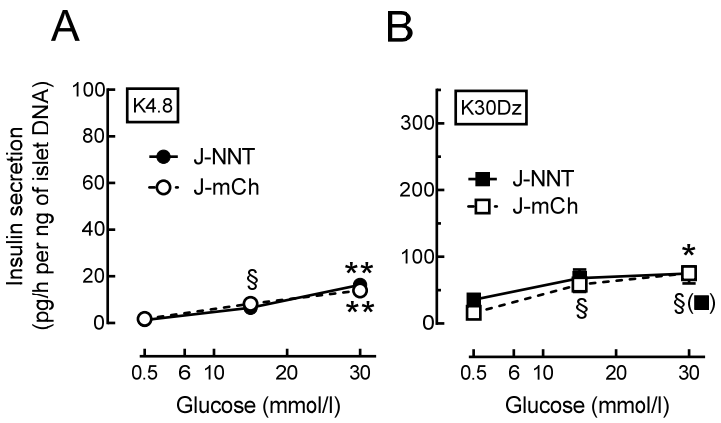

Figure S6. Metabolic amplification of insulin secretion in J-islets infected with Ad-NNT or Ad-mCh after gentle trypsinisation. Related to figure 5.

The islets were gently trypsinized before infection with Ad-NNT or Ad-mCh. They were then incubated as in figure 5. Islet DNA content (A, 0.49 ± 0.03 in J-NNT-islets and 0.49 ± 0.03 in J-mCh islets; B, 0.51 ± 0.08 in J-NNT-islets and 0.59 ± 0.02 in J-mCh-islets). Data are means ± SEM for 11-12 batches of 5 islets from 4 islet preparations. § P<0.05, * P<0.001, ** P<0.0001 *vs.* G0.5.

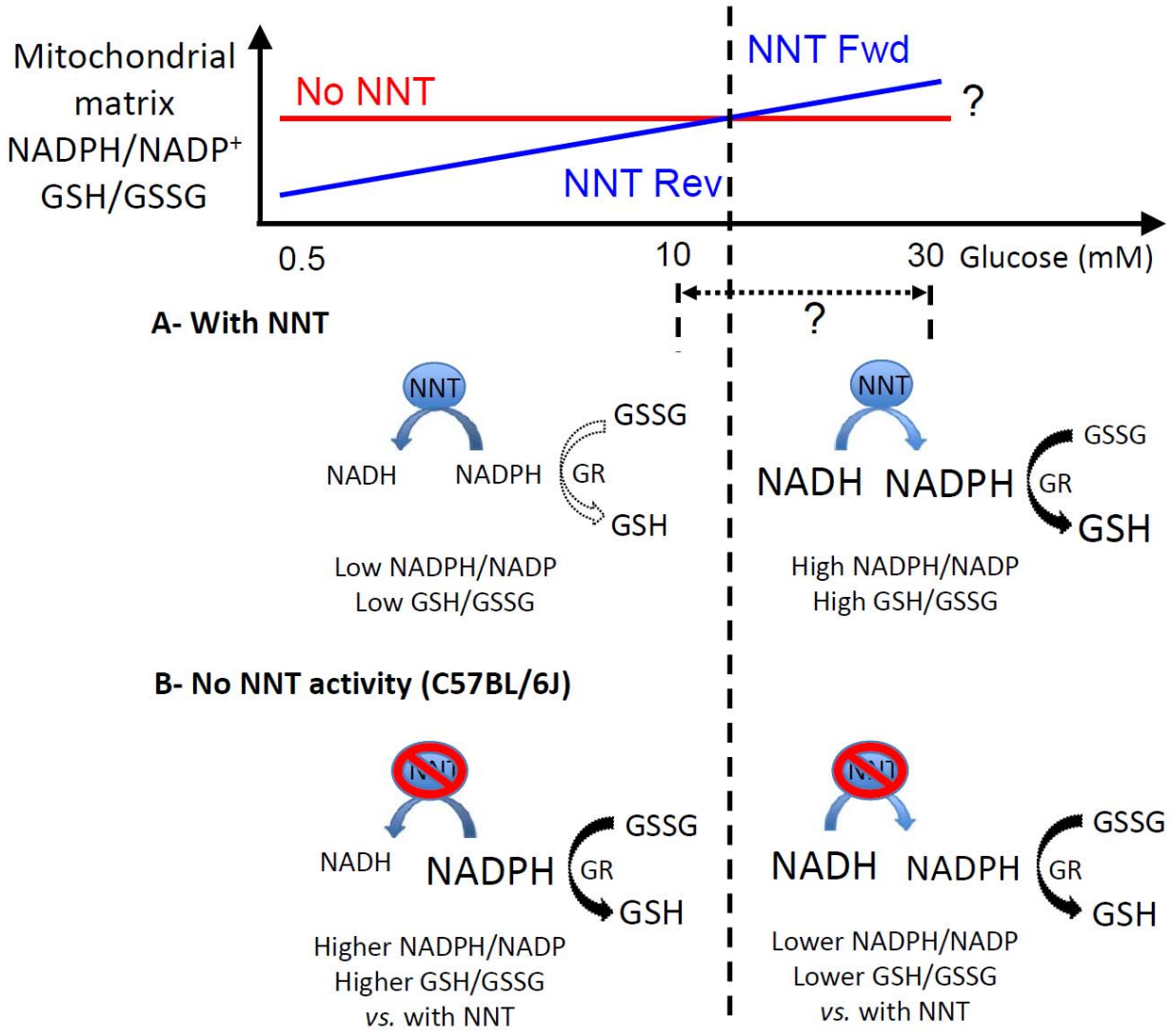

Figure S7. Model depicting the impact of NNT mode of operation on islet NADP and glutathione redox state at varying glucose concentrations. Related to figure 7.

GR, glutathione reductase. NNT Rev and NNT Fwd, reverse and forward mode of NNT operation. The differences in relative amount of oxidized and reduced pyridine nucleotides and glutathione are illustrated by the use of different font size. The horizontal dotted line between 10 and 30 mM glucose denotes the uncertainty regarding the glucose concentration at which NNT mode of operation switches from reverse to forward.